

TS-RIR: Translated synthetic room impulse responses for speech augmentation

Anton Ratnarajah¹, Zhenyu Tang¹, Dinesh Manocha¹

¹University of Maryland, College Park, MD 20742, United States

jeran@umd.edu, zhy@umd.edu, dmanocha@umd.edu

Abstract

We propose a method for improving the quality of synthetic room impulse responses generated using acoustic simulators for far-field speech recognition tasks. We bridge the gap between the synthetic room impulse responses and the real room impulse responses using our novel, one-dimensional CycleGAN architecture. We pass a synthetic room impulse response in the form of raw-waveform audio to our one-dimensional CycleGAN and translate it into a real room impulse response. We also perform sub-band room equalization to the translated room impulse response to further improve the quality of the room impulse response. We artificially create far-field speech by convolving the LibriSpeech clean speech dataset [1] with room impulse response and adding background noise. We show that far-field speech simulated with the improved room impulse response using our approach reduces the word error rate by up to 19.9% compared to the unmodified room impulse response in Kaldi LibriSpeech far-field automatic speech recognition benchmark [2].

Index Terms: geometric acoustic simulator, room equalization, domain adaptation, reverberation

1. Introduction

Far-field speech recognition is still a challenging problem because only a limited amount of the far-field speech corpus is available [3, 4]. Unlike near-field speech, which is recorded close to the microphone, far-field speech contains strong reverberation effects. The reverberation effects are associated with the room layout, speaker and listener position, and room materials. The reverberation effects can be mathematically modelled as a transfer function known as Room Impulse Response (RIR). We can simulate far-field speech by convolving clean speech with an RIR and adding environmental noise with different signal-to-noise ratios.

The RIR can be measured accurately from an acoustic environment using different techniques [5, 6, 7]. Recording RIRs requires a lot of human labor and special hardware. Alternatively, the RIR can be simulated using physically-based acoustic simulators for different scenes [8, 9, 10]. The current acoustic simulators have shown significant improvement in speech recognition tasks [11]. However, there is still a gap between the performance of RIRs generated using acoustic simulators and the performance of real RIRs. Most commonly used acoustic simulators are not capable of modelling all the acoustic effects present in the environment. For example, ray-tracing-based acoustic simulators [12, 11] make simulation errors at low frequencies due to ray assumptions. Inaccuracy in modelling RIRs using acoustic simulators causes performance gaps between real RIRs and synthetic RIRs in far-field automatic speech recognition (ASR) tasks.

In recent works, neural networks are used to translate

simple sketches without visual cues to photo-realistic images [13, 14]. Free-hand sketches are spatially imprecise and geometrically distorted [13]. CycleGAN [15] is capable of translating imprecise sketches to realistic photos. Motivated by the performance of CycleGAN in computer vision tasks, we implement a one-dimensional CycleGAN architecture to translate an imprecise RIR generated using an acoustic simulator to a real-world RIR. Our CycleGAN takes synthetic RIRs as audio samples to translate them into real RIRs.

Main Results: We improve the quality of synthetic RIRs using our one-dimensional CycleGAN and perform real-world sub-band room equalization to the improved RIRs. We show the benefit of our post-processed RIRs in far-field ASR systems. Our main contributions are as follows:-

- We present our one-dimensional CycleGAN, which is capable of translating an imprecise synthetic RIR to a real RIR.
- We propose a scheme to further improve the synthetic RIR by doing sub-band room equalization.
- We show that, on a modified Kaldi LibriSpeech far-field ASR benchmark [2], far-field speech simulated using our improved RIRs outperforms the far-field speech simulated using unmodified RIRs by up to 19.9 %.

The rest of the paper is organized as follows. In Section 2 we describe different acoustic simulation techniques and related works. We propose our novel approach to improve simulated RIRs in Section 3. Section 4 shows the benefit of improving synthetic RIRs in far-field ASR systems. Section 5 concludes the paper.

2. Related Work

2.1. Acoustic Simulation

There are several approaches for simulating RIRs for different acoustic environments. Among the existing methods, computing RIRs by numerically solving the wave equation gives the most accurate results for a given scene [8]. However, wave-based approaches are computationally expensive and do not scale well for complex scenes.

A simpler and less accurate alternative to the wave-based approach is geometric acoustic simulators [9, 11]. In geometric acoustic simulators, the sound is assumed to propagate as a ray instead of a wave. Therefore, wave properties of the sound are neglected in this simulator. The ray assumption is valid when the wavelength of the sound is significantly smaller than the size of the obstacle in the environment. However, significant simulation error is observed at low frequencies, where the wavelength is large. The image method [9] and path tracing methods [12, 16, 17, 11] are common geometric acoustic simulation methods. The image method is capable of only modelling spec-

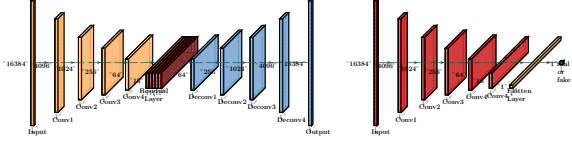


Figure 1: The generator (Left) and discriminator (Right) architecture of our one-dimensional CycleGAN.

ular reflections. Path tracing methods can model both specular and diffuse reflections.

We use a state-of-the-art geometric acoustic simulator [11] to generate RIRs for different scenes and improve the simulated synthetic RIR response using our novel approach for the far-field speech recognition task.

2.2. Techniques for improving synthetic RIR

The geometric acoustic simulators fail to model low-frequency wave effects such as diffraction [18] and room resonance [19] because of ray assumption. We observe a boost or diminish in the frequency response at different frequency bands in real RIRs due to room resonance. However, the frequency response of synthetic RIRs simulated using a geometric acoustic simulator is mostly flat. In a prior work [2], missing room resonance is compensated in synthetic RIRs using a real-world sub-band room equalization approach.

In recent works, CycleGAN [15] has shown impressive results in transferring style from one image to another image while preserving the details in the input image. In our work, we aim to transfer low-frequency wave effects from real RIRs to synthetic RIRs using CycleGAN. We also combine the prior method [2] with our proposed method to improve the quality of synthetic RIRs. Our approach reduces the performance gap between synthetic RIRs and real RIRs in far-field automatic speech recognition tasks.

3. Proposed Method

3.1. Translation: Synthetic RIR \Rightarrow Real RIR

We design a one-dimensional CycleGAN architecture to learn mapping functions between synthetic RIRs (S) and real RIRs (R) in the absence of paired training examples. Inspired by WaveGAN [20], which applies generative adversarial networks (GANS) to raw-waveform audio, we directly input RIRs as raw audio samples to our network to learn the mapping functions. In most cases, RIRs are less than one second in duration. Therefore, we re-sample the synthetic and real RIR dataset to 16 kHz and pass them as a one-dimensional input of length 16384.

We represent the real RIR training samples as $\{r_i\}_{i=1}^N$ where $r_i \in R$ and the synthetic RIR training samples as $\{s_i\}_{i=1}^N$ where $s_i \in S$. The data distributions of the training samples are $r \sim p_{data}(r)$ and $s \sim p_{data}(s)$. We use 2 generators to learn the mappings $G_{SR} : S \rightarrow R$ and $G_{RS} : R \rightarrow S$. We use discriminator D_R to differentiate real RIRs $\{r_i\}_{i=1}^N$ and synthetic RIRs translated to real RIRs $\{G_{SR}(s_i)\}_{i=1}^N$. Similarly, we use D_S to discriminate $\{s_i\}_{i=1}^N$ and $\{G_{RS}(r_i)\}_{i=1}^N$. Our objective function contains adversarial loss [21], cycle-consistency loss [22] and identity loss [23] to learn the mapping functions.

3.1.1. Adversarial Loss

To ensure the synthetic RIRs are translated to real RIRs, the following objective is used for the mapping function $G_{SR} : S \rightarrow R$ and the discriminator D_R .

$$\mathcal{L}_{adv}(G_{SR}, D_R, S, R) = \mathbb{E}_{r \sim p_{data}(r)}[\log D_R(r)] + \mathbb{E}_{s \sim p_{data}(s)}[\log(1 - D_R(G_{SR}(s)))] \quad (1)$$

The discriminator D_R tries to distinguish between translated RIRs using the mapping function $G_{SR} : S \rightarrow R$ from the real RIRs by maximizing the loss. The generator $G_{SR} : S \rightarrow R$ attempts to generate real RIRs that fools D_R by minimizing the loss, i.e., $\min_{G_{SR}} \max_{D_R} \mathcal{L}_{adv}(G_{SR}, D_R, S, R)$. Similarly, we train the mapping function $G_{RS} : R \rightarrow S$ and the discriminator D_S with the objective $\mathcal{L}_{adv}(G_{RS}, D_S, R, S)$.

3.1.2. Cycle Consistency Loss

We use cycle consistency loss to preserve the details in the RIRs during the translation. The cycle consistency loss (Equation 2) ensures that $G_{RS}(G_{SR}(s)) \sim s$ and $G_{SR}(G_{RS}(r)) \sim r$.

$$\mathcal{L}_{cyc}(G_{SR}, G_{RS}) = \mathbb{E}_{s \sim p_{data}(s)}[\|G_{RS}(G_{SR}(s)) - s\|_1] + \mathbb{E}_{r \sim p_{data}(r)}[\|G_{SR}(G_{RS}(r)) - r\|_1] \quad (2)$$

3.1.3. Identity Mapping Loss

We preserve the input RIR using the identity mapping loss:

$$\mathcal{L}_{id}(G_{SR}, G_{RS}) = \mathbb{E}_{s \sim p_{data}(s)}[\|G_{RS}(s) - s\|_1] + \mathbb{E}_{r \sim p_{data}(r)}[\|G_{SR}(r) - r\|_1] \quad (3)$$

3.1.4. Full Objective

Equation 4 shows our full objective function.

$$\begin{aligned} \mathcal{L}(G_{SR}, G_{RS}, D_S, D_R) = & \mathcal{L}_{adv}(G_{SR}, D_R, S, R) \\ & + \mathcal{L}_{adv}(G_{RS}, D_S, R, S) \\ & + \lambda_{cyc} \mathcal{L}_{cyc}(G_{SR}, G_{RS}) \\ & + \lambda_{id} \mathcal{L}_{id}(G_{SR}, G_{RS}), \end{aligned} \quad (4)$$

where λ_{cyc} and λ_{id} controls the relative importance of cycle consistency loss and identity mapping loss respectively. We train our one-dimensional CycleGAN to find the optimal mapping functions G_{SR}^* and G_{RS}^* by solving

$$G_{SR}^*, G_{RS}^* = \arg \min_{G_{SR}, G_{RS}} \max_{D_S, D_R} \mathcal{L}(G_{SR}, G_{RS}, D_S, D_R) \quad (5)$$

We use G_{SR}^* to translate imprecise synthetic RIRs to real RIRs.

3.1.5. Implementation

Network Architecture: We adapt the discriminator architecture from Donahue et al.[20] who have shown impressive results in synthesizing raw-waveform audio. We did not use the phase shuffle operation proposed in Donahue et al.[20] because this operation did not improve our results. Inspired by Johnson et

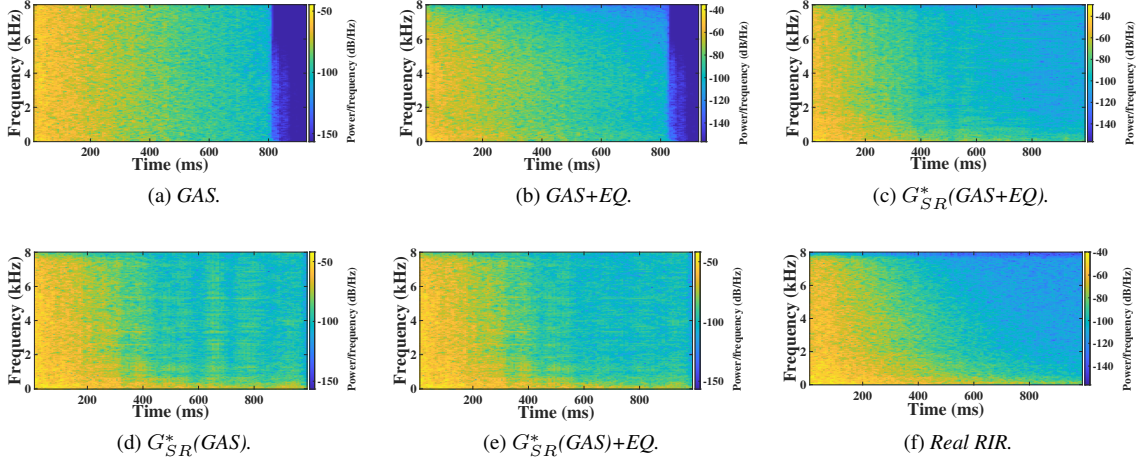


Figure 2: The spectrogram of a synthetic RIR generated using the state-of-the-art geometric acoustic simulator, post-processed synthetic RIRs, and a real RIR. Sub-band room equalization (EQ) and synthetic RIR to real RIR (G_{SR}^* ()) translation are the two methods used to post-process the synthetic RIR.

al. [24], we designed our generator network consisting of an encoder, a transformer and a decoder. Figure 1 describes our generator and discriminator architecture. We use one-dimensional filters of length 25 to perform convolution and transposed convolution operations in our one-dimensional CycleGAN architecture.

Dataset: We use equal amount of real-world RIRs from BUT ReverbDB [25] and synthetic RIRs generated using the state-of-the-art geometric acoustic simulator to train our one-dimensional CycleGAN architecture. The BUT ReverbDB consists of 1891 RIRs covering the office, hotel room, conference room, lecture room, meeting room and stairs. We remove repeated RIRs and RIRs generated from environments that are difficult to simulate using acoustic simulators and retain the remaining 1209 RIRs. Among 1209 RIRs, we train our network using 967 RIRs and keep 242 RIRs for testing purpose.

3.2. Sub-band Room Equalization

Sub-band room equalization bridges the gap in the frequency gain of real-world and simulated RIRs. We adapt the sub-band room equalization approach proposed in [2]. Sub-band relative gain calculation and equalization matching are the two stages in sub-band room equalization.

3.2.1. Sub-band relative gain calculation

We calculate the frequency response of every RIR in a real-world dataset [25]. We compute the relative gain from the frequency response by taking the gain at 1000Hz as the reference for each real RIR. Then we extract the relative frequency gain at 7 unique sample points (62.5Hz, 125Hz, 250Hz, 500Hz, 2000Hz, 4000Hz, 8000Hz) for every real RIR. The relative gain of the sampled points varies with different mean and standard deviations. We use the Gaussian mixture model to model 7 Gaussian distributions using the relative gains from the sampled points. We resample equal number of relative gains for each sample point as the input to the Gaussian mixture model. Instead of using the relative gains of the real RIRs, we use the resampled relative gains. We use resampled relative gains to avoid duplicating the real RIRs during equalization matching.

We use the resampled relative gains to compensate for the difference in relative gains between synthetic and real RIRs.

3.2.2. Equalization matching

We compute the relative frequency gains for the synthetic RIRs generated using the state-of-the-art geometric acoustic simulator at the chosen sample points (62.5Hz, 125Hz, 250Hz, 500Hz, 2000Hz, 4000Hz, 8000Hz), taking gain at 1000Hz as the reference. We calculate the difference in the relative gains of synthetic RIRs and the re-sampled relative gains. Then we design a finite impulse response (FIR) filter using the window method [26] to compensate for the difference in the relative gains. We filter the synthetic RIRs using our designed FIR filter to match the sub-band relative gains of synthetic RIRs with the real RIRs.

3.3. Optimal Combination

We translate synthetic RIRs to real RIRs (G_{SR}^* ()) and do sub-band room equalization (EQ) to improve the quality of synthetic RIRs simulated using the state-of-the-art geometric acoustic simulator (GAS). We tried different combinations of our post-processing approach to come up with the optimal combination (Table 1). Figure 2 shows the spectrogram of a synthetic RIR simulated using the state-of-the-art geometric acoustic simulator, post-processed synthetic RIRs using a different combination of our post-processing approach and a real RIR. From the spectrograms, we can see that by translating a synthetic RIR to a real RIR, we improve the energy distribution in the low-frequency region (Figure 2d). When we do sub-band room equalization after translation, we observe further refinement in the spectrogram (Figure 2e), especially around 600ms to 800ms.

4. Experiment and Results

4.1. Benchmark

We evaluate our approach on the Kaldi LibriSpeech far-field ASR recipe [2]. We convolve clean speech $x_c[t]$ from LibriSpeech [1] with different sets of RIRs $r[t]$ and add environmental noise $n[t]$ from BUT ReverbDB [25] to simulate a far-

Table 1: *Different combinations of our post-processing methods studied in this paper.*

Combination	Description
GAS+EQ	Only perform room equalization.
G_{SR}^* (GAS+EQ)	First, perform room equalization, then translate the equalized synthetic RIR to a real RIR.
G_{SR}^* (GAS)	Only translate synthetic RIR to real RIR.
G_{SR}^* (GAS)+EQ	First, translate a synthetic RIR to a real RIR, then do room equalization to the translated RIR.

field speech $x_f[t]$ training dataset. The environmental noise is started at a random position l and repeated in a loop to fill the clean speech. In Equation 6, λ is calculated for different signal-to-noise ratios. The signal-to-noise ratio used in the benchmark ranges from 1dB to 2dB.

$$x_f[t] = x_c[t] \circledast r[t] + \lambda * n[t+l]. \quad (6)$$

We train time-delay neural networks [27] using our simulated training dataset. After training the network, we decode the i-vectors of a real-world far-field speech test set using phone language models. We calculate word error rate for large four-gram (fglarge), large tri-gram (tqlarge), medium tri-gram (tgmed), and small tri-gram (tgsmall) phone language models, and we use online decoding using a tgsmall phone language model to evaluate the far-field speech simulated using different sets of RIRs. In online decoding, the i-vectors extracted from the real-world far-field speech test set are passed in real-time.

Training and testing on the benchmark for each simulated far-field speech training dataset take around 4 days. We used 32 Intel(R) Xeon(R) Silver 4208 CPUs @ 2.10 GHz and 2 GeForce RTX 2080 Ti GPUs to run the benchmark. We ran all the experiments on the same hardware for a fair comparison.

4.2. Data Preparation

We use real-world RIRs and environmental noise from BUT ReverbDB [25] and clean speech (test-clean) from LibriSpeech [1] to augment a real-world far-field speech test set using Equation 6. We evaluate our proposed method using the real-world far-field speech test set. We randomly split 1209 RIRs in BUT ReverbDB [25] into subsets of $\{773, 194, 242\}$ to create training, development, and test sets.

We use the meta-info accompanying with each real-world RIR to simulate synthetic RIRs using the state-of-the-art geometric acoustic simulator (GAS). We post-process the simulated RIRs by translating synthetic RIRs to real RIRs and performing real-world sub-band room equalization in different combinations (Table 1). Table 2 provides detailed information on different far-field speech training sets used for our evaluation. We use the environmental noise from BUT ReverbDB [25] and create our far-field speech training set using Equation 6.

4.3. Results and Analysis

Table 3 shows the word error rate (WER) reported by the Kaldi LibriSpeech far-field ASR benchmark [2]. We can see that the simulated far-field speech training sets perform well compared to our baseline model trained on a clean LibriSpeech dataset. The lowest WER is reported by our oracle model trained on

Table 2: *Training dataset overview. REMOVE THIS TABLE*

Dataset	RIR	#RIRs	LibriSpeech dataset
train-real	But ReverbDB	773	train-clean- $\{100, 360\}$
train-clean	None	0	train-clean- $\{100, 360\}$
train-GAS	GAS	773	train-clean- $\{100, 360\}$
train-GAS.E	GAS+EQ	773	train-clean- $\{100, 360\}$
train-T(GAS.E)	G_{SR}^* (GAS+EQ)	773	train-clean- $\{100, 360\}$
train-T(GAS)	G_{SR}^* (GAS)	773	train-clean- $\{100, 360\}$
train-T(GAS).E	G_{SR}^* (GAS)+EQ	773	train-clean- $\{100, 360\}$

Table 3: *Word error rate (WER) reported by the Kaldi LibriSpeech far-field ASR system. We trained the Kaldi model using the different simulated far-field speech training sets and tested it on a real-world far-field speech. We report WER for fqlarge, tqlarge, tgmed, and tgsmall phone language models and online decoding using tgsmall phone language model.*

Training data	Test Word Error Rate (WER) [%]				
	fqlarge	tqlarge	tgmed	tgsmall	online
real (Baseline)	77.15	77.37	78.00	78.94	79.00
clean (Oracle)	12.40	13.19	15.62	16.92	16.88
GAS [11]	16.53	17.26	20.24	21.91	21.83
GAS.E [2]	14.51	15.37	18.33	20.01	19.99
T(GAS.E)	14.27	14.98	17.79	19.37	19.36
Ours	T(GAS)	14.12	14.70	17.44	19.08
	T(GAS).E	13.24	14.04	16.65	18.40
					18.39

real-world far-field speech. In our work, we aim to minimize the gap in the performance between real-world RIRs and synthetic RIRs.

In prior work [2], real-world sub-band room equalization is used to improve the quality of synthetic RIRs. In this work, we propose an approach to translate imprecise synthetic RIRs to real RIRs. The WERs for tgsmall reported by train-GAS.E and train-T(GAS) are 18.33% and 17.44% respectively. We can see that our approach outperforms the prior work by up to 4.8%. We see an interesting observation with train-T(GAS.E) and train-T(GAS) datasets. When compared to translated synthetic RIRs, translated room equalized RIRs perform poorly.

Optimal Approach: We can see that translating imprecise synthetic RIRs to real RIRs and performing real-world sub-band room equalization on the translated RIRs (train-T(GAS).E) gives the lowest WER. When compared to training sets created using unmodified RIRs (train-GAS) and room equalized RIRs (train-GAS.E), we observe a relative reduction in WER by up to 19.9% and 9.1%, respectively.

5. Conclusion

In this paper, we propose a method to translate imprecise synthetic RIRs to real RIRs. We translate synthetic RIRs to real RIRs using our proposed method and perform real-world sub-band room equalization on the translated RIRs to improve the quality of synthetic RIRs. We evaluate this post-processing approach on the Kaldi LibriSpeech far-field automatic speech recognition benchmark. We show that our post-processing scheme outperforms unmodified synthetic RIRs by up to 19.9% and improved synthetic RIRs using the prior technique [2] by up to 9.1%.

6. References

- [1] V. Panayotov, G. Chen, D. Povey, and S. Khudanpur, "LibriSpeech: An asr corpus based on public domain audio books," in *2015 IEEE International Conference on Acoustics, Speech and Signal Processing (ICASSP)*, 2015, pp. 5206–5210.
- [2] Z. Tang, H. Meng, and D. Manocha, "Low-frequency compensated synthetic impulse responses for improved far-field speech recognition," in *2020 IEEE International Conference on Acoustics, Speech and Signal Processing, ICASSP 2020, Barcelona, Spain, May 4-8, 2020*. IEEE, 2020, pp. 6974–6978. [Online]. Available: <https://doi.org/10.1109/ICASSP40776.2020.9054454>
- [3] C. Richey, M. A. Barrios, Z. Armstrong, C. Bartels, H. Franco, M. Graciarena, A. Lawson, M. K. Nandwana, A. Stauffer, J. van Hout, P. Gamble, J. Hetherly, C. Stephenson, and K. Ni, "Voices obscured in complex environmental settings (voices) corpus," 2018.
- [4] J. Garofolo, C. Laprun, and J. Fiscus, "The rich transcription 2004 spring meeting recognition evaluation," 2004-04-01 2004.
- [5] M. R. Schroeder, "Integrated-impulse method measuring sound decay without using impulses," *The Journal of the Acoustical Society of America*, vol. 66, no. 2, pp. 497–500, 1979.
- [6] N. Aoshima, "Computer-generated pulse signal applied for sound measurement," *The Journal of the Acoustical Society of America*, vol. 69, no. 5, pp. 1484–1488, 1981.
- [7] A. Farina, "Advancements in impulse response measurements by sine sweeps," in *Audio Engineering Society Convention 122*, May 2007. [Online]. Available: <http://www.aes.org/e-lib/browse.cfm?elib=14106>
- [8] N. Raghuvanshi, R. Narain, and M. C. Lin, "Efficient and accurate sound propagation using adaptive rectangular decomposition," *IEEE Transactions on Visualization and Computer Graphics*, vol. 15, no. 5, pp. 789–801, 2009.
- [9] J. B. Allen and D. A. Berkley, "Image method for efficiently simulating small-room acoustics," *Acoustical Society of America Journal*, vol. 65, no. 4, pp. 943–950, Apr. 1979.
- [10] T. Ko, V. Peddinti, D. Povey, M. L. Seltzer, and S. Khudanpur, "A study on data augmentation of reverberant speech for robust speech recognition," in *2017 IEEE International Conference on Acoustics, Speech and Signal Processing (ICASSP)*, 2017, pp. 5220–5224.
- [11] Z. Tang, L. Chen, B. Wu, D. Yu, and D. Manocha, "Improving reverberant speech training using diffuse acoustic simulation," in *ICASSP 2020 - 2020 IEEE International Conference on Acoustics, Speech and Signal Processing (ICASSP)*, 2020, pp. 6969–6973.
- [12] C. Schissler and D. Manocha, "Interactive sound propagation and rendering for large multi-source scenes," *ACM Trans. Graph.*, vol. 36, no. 1, Sep. 2016. [Online]. Available: <https://doi.org/10.1145/2943779>
- [13] R. Liu, Q. Yu, and S. X. Yu, "Unsupervised sketch to photo synthesis," in *Computer Vision - ECCV 2020 - 16th European Conference, Glasgow, UK, August 23-28, 2020, Proceedings, Part III*, ser. Lecture Notes in Computer Science, A. Vedaldi, H. Bischof, T. Brox, and J. Frahm, Eds., vol. 12348. Springer, 2020, pp. 36–52. [Online]. Available: https://doi.org/10.1007/978-3-030-58580-8_3
- [14] H. Kazemi, F. Taherkhani, and N. M. Nasrabadi, "Unsupervised facial geometry learning for sketch to photo synthesis," in *2018 International Conference of the Biometrics Special Interest Group, BIOSIG 2018, Darmstadt, Germany, September 26-28, 2018*, ser. LNI, A. Brömmel, C. Busch, A. Dantcheva, C. Rathgeb, and A. Uhl, Eds., vol. P-282. GI / IEEE, 2018, pp. 1–5. [Online]. Available: <https://doi.org/10.23919/BIOSIG.2018.8552937>
- [15] J. Zhu, T. Park, P. Isola, and A. A. Efros, "Unpaired image-to-image translation using cycle-consistent adversarial networks," in *IEEE International Conference on Computer Vision, ICCV 2017, Venice, Italy, October 22-29, 2017*. IEEE Computer Society, 2017, pp. 2242–2251. [Online]. Available: <https://doi.org/10.1109/ICCV.2017.244>
- [16] M. T. Taylor, A. Chandak, Q. Mo, C. Lauterbach, C. Schissler, and D. Manocha, "Guided multiview ray tracing for fast auralization," *IEEE Trans. Vis. Comput. Graph.*, vol. 18, no. 11, pp. 1797–1810, 2012. [Online]. Available: <https://doi.org/10.1109/TVCG.2012.27>
- [17] M. T. Taylor, A. Chandak, L. Antani, and D. Manocha, "Resound: interactive sound rendering for dynamic virtual environments," in *Proceedings of the 17th International Conference on Multimedia 2009, Vancouver, British Columbia, Canada, October 19-24, 2009*, W. Gao, Y. Rui, A. Hanjalic, C. Xu, E. G. Steinbach, A. El-Saddik, and M. X. Zhou, Eds. ACM, 2009, pp. 271–280. [Online]. Available: <https://doi.org/10.1145/1631272.1631311>
- [18] R. R. Torres, U. P. Svensson, and M. Kleiner, "Computation of edge diffraction for more accurate room acoustics auralization," *The Journal of the Acoustical Society of America*, vol. 109, no. 2, pp. 600–610, 2001. [Online]. Available: <https://doi.org/10.1121/1.1340647>
- [19] Z. Tang, N. J. Bryan, D. Li, T. R. Langlois, and D. Manocha, "Scene-aware audio rendering via deep acoustic analysis," *IEEE Trans. Vis. Comput. Graph.*, vol. 26, no. 5, pp. 1991–2001, 2020. [Online]. Available: <https://doi.org/10.1109/TVCG.2020.2973058>
- [20] C. Donahue, J. J. McAuley, and M. S. Puckette, "Adversarial audio synthesis," in *7th International Conference on Learning Representations, ICLR 2019, New Orleans, LA, USA, May 6-9, 2019*. OpenReview.net, 2019. [Online]. Available: <https://openreview.net/forum?id=ByMVTsR5KQ>
- [21] I. J. Goodfellow, J. Pouget-Abadie, M. Mirza, B. Xu, D. Warde-Farley, S. Ozair, A. Courville, and Y. Bengio, "Generative adversarial nets," in *Proceedings of the 27th International Conference on Neural Information Processing Systems - Volume 2*, ser. NIPS'14. Cambridge, MA, USA: MIT Press, 2014, p. 2672–2680.
- [22] T. Zhou, P. Krähenbühl, M. Aubry, Q. Huang, and A. A. Efros, "Learning dense correspondence via 3d-guided cycle consistency," in *2016 IEEE Conference on Computer Vision and Pattern Recognition, CVPR 2016, Las Vegas, NV, USA, June 27-30, 2016*. IEEE Computer Society, 2016, pp. 117–126. [Online]. Available: <https://doi.org/10.1109/CVPR.2016.20>
- [23] Y. Taigman, A. Polyak, and L. Wolf, "Unsupervised cross-domain image generation," in *5th International Conference on Learning Representations, ICLR 2017, Toulon, France, April 24-26, 2017, Conference Track Proceedings*. OpenReview.net, 2017. [Online]. Available: <https://openreview.net/forum?id=Sk2Im59ex>
- [24] J. Johnson, A. Alahi, and L. Fei-Fei, "Perceptual losses for real-time style transfer and super-resolution," in *Computer Vision - ECCV 2016 - 14th European Conference, Amsterdam, The Netherlands, October 11-14, 2016, Proceedings, Part II*, ser. Lecture Notes in Computer Science, B. Leibe, J. Matas, N. Sebe, and M. Welling, Eds., vol. 9906. Springer, 2016, pp. 694–711. [Online]. Available: https://doi.org/10.1007/978-3-319-46475-6_43
- [25] I. Szöke, M. Skácel, L. Mošner, J. Palísek, and J. Černocký, "Building and evaluation of a real room impulse response dataset," *IEEE Journal of Selected Topics in Signal Processing*, vol. 13, no. 4, pp. 863–876, 2019.
- [26] S. W. Smith, *The Scientist and Engineer's Guide to Digital Signal Processing*. USA: California Technical Publishing, 1997.
- [27] V. Peddinti, D. Povey, and S. Khudanpur, "A time delay neural network architecture for efficient modeling of long temporal contexts," in *INTERSPEECH 2015, 16th Annual Conference of the International Speech Communication Association, Dresden, Germany, September 6-10, 2015*. ISCA, 2015, pp. 3214–3218. [Online]. Available: http://www.isca-speech.org/archive/interspeech_2015/i15_3214.html